Torque control of a shunt wound and DC motor of an electric vehicle by means of continuous field control and stepwise adjustment of the armature voltage

full battery voltage to the motor terminals and the vehicle speed can be controlled by variation of the field current.
Yet the use of a multi-speed gearbox has the following advantages (**Fig. 8**):

- during the starting phase a higher gear ratio can be engaged, which reduces the initial current drawn from the battery
- with the possibility of selecting different gear ratios it is easier to meet demands for hill climbing
- since separately excited dc motors are less efficient at low rotational speeds, variable gear ratios allow highly efficient motor operation.

A thyristor chopper for the armature circuit is being developed which will control the Siemens motor coupled to either the step-down gear or the automatic gearbox.
The efficiency of these approaches appears to be high, since the losses in the motor controller are small and regenerative braking is possible. Other advantages are operational comfort and acceptable range. A disadvantage of these drive systems is the costly armature controller, which must be able to handle currents up to the 350 Ampere.

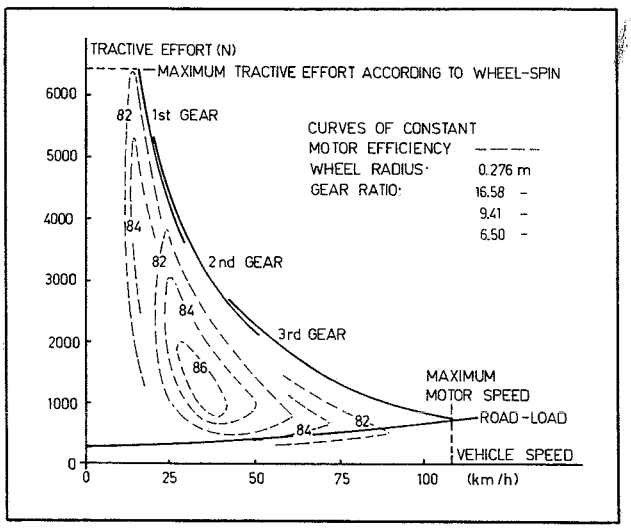

Fig. 8 Fully electronic motor control and a multi-speed gearbox

REFERENCES

[1] W. H. M. Visscher, W. de Zeeuw, R van der Graaf: Experiments on Lead-Acid Batteries of an Electric Vehicle
EVS-5 Philadelphia, Oct. 1978.

[2] W. A. Koumans: The Electric Car Project of the Eindhoven University of Technology
PPL Conference Publication, no. 14.

[3] L. A. M. van Dongen, R. van der Graaf, W. H. M. Visscher: Theoretical Prediction of Electric Vehicle Energy Consumption and Battery State-of-Charge during Arbitrary Driving Cycles.
EVC Symposium VI, Baltimore, Oct. 1981.

[4] H. C. J. Zeegers: Torque control of a shunt wound dc-motor of an electric vehicle by means of continuous field control and stepwise adjustment of the armature voltage.
Drive Electric Amsterdam '82 Oct. 1982

[5] Leo A. M. van Dongen: Efficiency Characteristics of Manual and Automatic Passenger Car Transaxles.
Society of Automotive Engineers, paper 820741. Troy, Michigan, June 1982.

[6] S. W. M. van Vuuren: Analyse van een stadsrit. Eindhoven University of Technology, Dept. of Mech. Eng. Internal report.

Torque control of a shunt wound DC motor of an electric vehicle by means of continuous field control and stepwise adjustment of the armature voltage [1])

ABSTRACT

It is shown that notching armature voltage and continuous field control can be a compromise solution for EV-drives. For the given vehicle parameters the necessarily series resistors are determined. An analysis of field control at different armature voltages is given for both stationary and dynamic conditions. Flow chart and block diagram of the control system are given. Attention is paid to the MOSFET-implemented field controllers and to the measurement of the electromagnetic torque using armature and field current.

by H. C. J. Zeegers [2])

1. Introduction

In the early seventies a group at the university of Eindhoven started to work on the subject of electrically driven vehicles in order to provide authorities with reliable data in this field. In 1973 it was decided to develop an electric passenger car.

1.1. The EV of the Eindhoven University of Technology

The vehicle should meet the following requirements [7]:

1. capacity: 2 adults + 2 children (so called 2+2 car);
2. range: 100 km;
3. topspeed: approx. 90 km/h;
4. cruising speed: 50-70 km/h;
5. acceleration: 1.5 m/S^2 up till 50 km/h;
6. gradients: 20% at stall condition;
7. rapidly exchangeable battery pack;
8. active safety (good road-holding, handling and suspension);
9. good passive safety considering the presence of the battery pack;
10. the electric drive should be such that it offers high efficiency and makes the car easy and pleasant to drive, also for persons used to cars with internal combustion engine. Besides that it should be cheap and servicing should be easy to be carried out by garage personnel with little extra training;
11. regenerative breaking.

After research by the groups transport research [3], [4] and electrochemistry [4], [10], it was decided to modify a VW-Rabbit car and equip it with a 120 V - 240 Ah lead-acid battery. The battery pack is made up of twenty 6 V-batteries. This concept resulted in a total vehicle weight of approximately 1500 kg.
Taking into consideration the requirements for the electrical drive (see point 10), it was concluded that while an armature-chopper has the advantage of easy control and good effi-

[1]) Paper gepresenteerd tijdens 'Drive Electric 1982' te Amsterdam

[2]) Eindhoven University of Technology, Eindhoven, The Netherlands.

ciency, it has the disadvantage of being expensive and containing a lot of advanced electronics. It was expected that stepwise armature voltage adjustment with field control in addition would offer a good compromise solution. In order to verify this statement both systems should be investigated. The following program was started:

A. Development of a system based upon stepwise armature voltage adjustment by means of electromagnetic switches and continuous field control by a transistor chopper. At very low speeds additional armature resistors are required.

B. Development of a system with an armature **and** field current chopper.

C. Comparison of A. and B.

This paper deals with part A. of the project. To realize A. a fixed reduction between machine shaft and wheels of 7.6 had to be considered, which means that the machine speed must be controlled over a large range. Driving backwards is possible by reversing the field current. In order to realize regenerative breaking, with this circuit configuration it is best to use a DC-machine with separate excitation.

A Siemens-machine, type 1GV1 appeared to be the most suitable traction machine commercially available. Nominal and maximum values are specified in table 1 [9].

Mechanical and electrical performances are shown in **fig. 1a and 1b**.

TABLE 1

	Nominal	Maximum
Armature voltage	130 V (at nom.motor cond.)	180 V
Armature current	150 A	320 A (3 min)
Excitation voltage	100 V	—
Excitation current	7 A	—
Speed	2200 min^{-1}	6700 min^{-1}
Torque	75 Nm	160 Nm
Power	17 kW	33.5 kW

1.2. Speed control of the separately excited DC-machine

A seperately excited DC-machine offers two gates, named armature and field winding terminals, through which it can be controlled.

Fig. 2. shows a machine connected to a voltage source U and loaded with a torque T_L plus friction torque T_{fr}.

The total inertia of armature plus load is called J.

This drive can be described by the following equations:

$$U = I_a R_a + L_a \frac{dI_a}{d\tau} + E + \frac{I_a}{|I_a|} U_b \qquad (1)$$

$$E = c_m \Omega \Phi_a \qquad (2)$$

$$T_e = c_m I_a \Phi_a \qquad (3)$$

$$T_e = T_L + T_{fr} + J \frac{d\Omega}{d\tau} \qquad (4)$$

$$U_f = \frac{d\Phi_s}{d\tau} + I_f R_f \qquad (5)$$

Due to leakage, Φ_s and Φ_a differ slightly.

If we consider the system under quasi-stationary conditions ($\frac{dI_a}{d\tau} \approx 0, \frac{d\Omega}{d\tau}$ is small) and if we neglect the armature reaction and the voltage drop U_b across the brushes, which

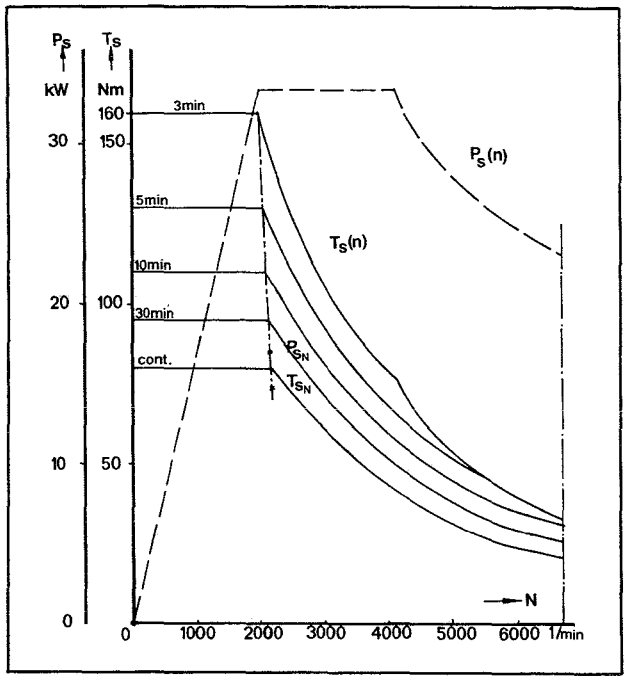

Fig. 1a The mechanical performances of the 1GV1

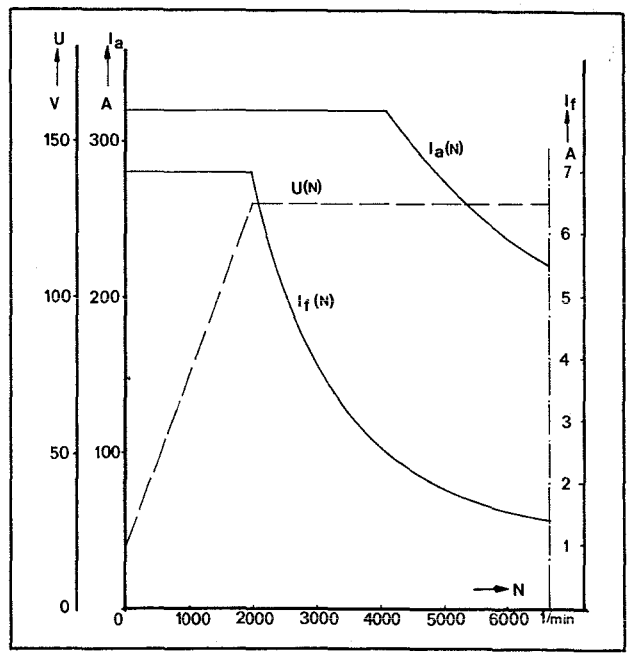

Fig. 1b The electrical performances of the 1GV1

is mostly 1 - 1.5 V, the equation of motion can be derived from (1), (2) and (3). This gives the relationship between electromagnetic torque T_e and angular speed Ω.

$$T_e = \frac{c_m \Phi_a}{R_a} (U - c_m \Omega \Phi_a) \qquad (6)$$

A general relation is found when the parameters are made dimensionless. Relating the magnitudes to their nominal values [6] we get:

$$t_e = \frac{T_e}{T_{eN}} = \frac{T_e}{c_m \Phi_{a_N} I_{a_N}} \qquad (7)$$

$$\omega = \frac{\Omega}{\Omega_N} \tag{8}$$

$$u = \frac{U}{U_N} = \frac{U}{c_m \Phi_{a_N} \Omega_N} \tag{9}$$

$$\varphi = \frac{\Phi_a}{\Phi_{a_N}} \tag{10}$$

$$r = \frac{R_a}{R_N} = \frac{R_a}{U_N / I_{a_N}} \tag{11}$$

One must be aware of the fact that U_N is defined as armature voltage under no-load conditions at nominal speed and nominal excitation. This value differs from the one given by the manufacturers for nominal motor conditions. The magitude $R_N = \frac{U_N}{I_{a_N}}$ is a fictive value which proves to be convenient once introduced. By using (6) up to (11) the general equation of motion is obtained.

$$t_e = \frac{u\varphi}{r} - \frac{\omega \varphi^2}{r} \tag{12}$$

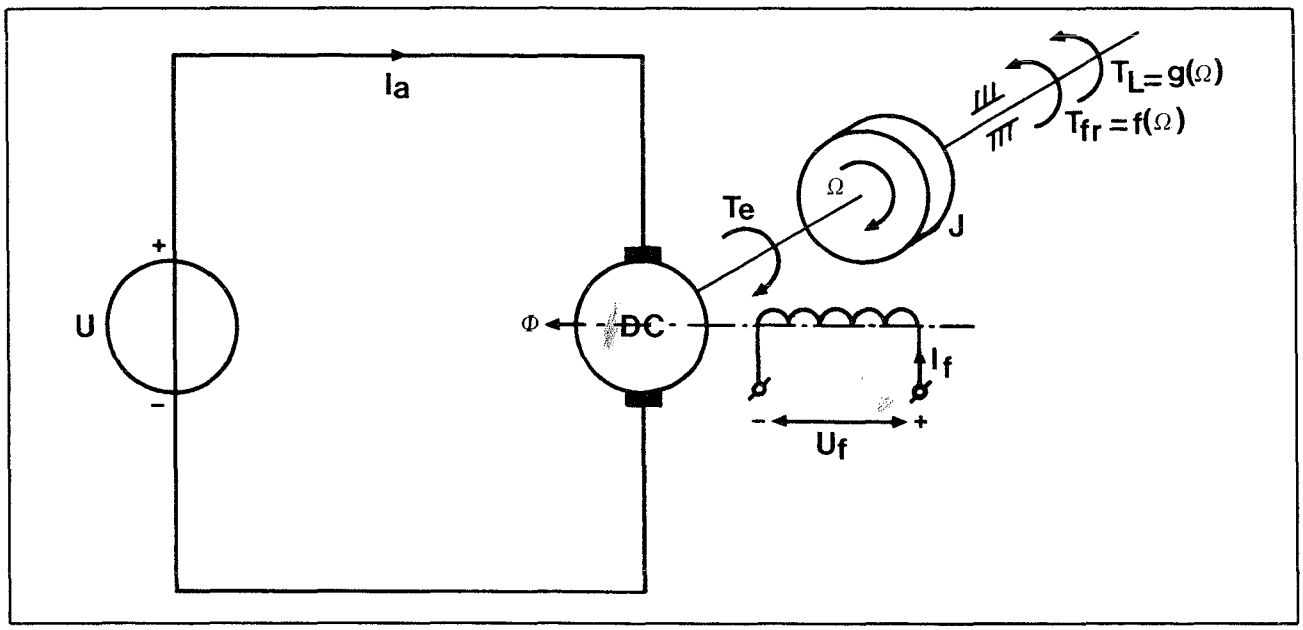

Fig. 2 Electrical drive with a DC-machine

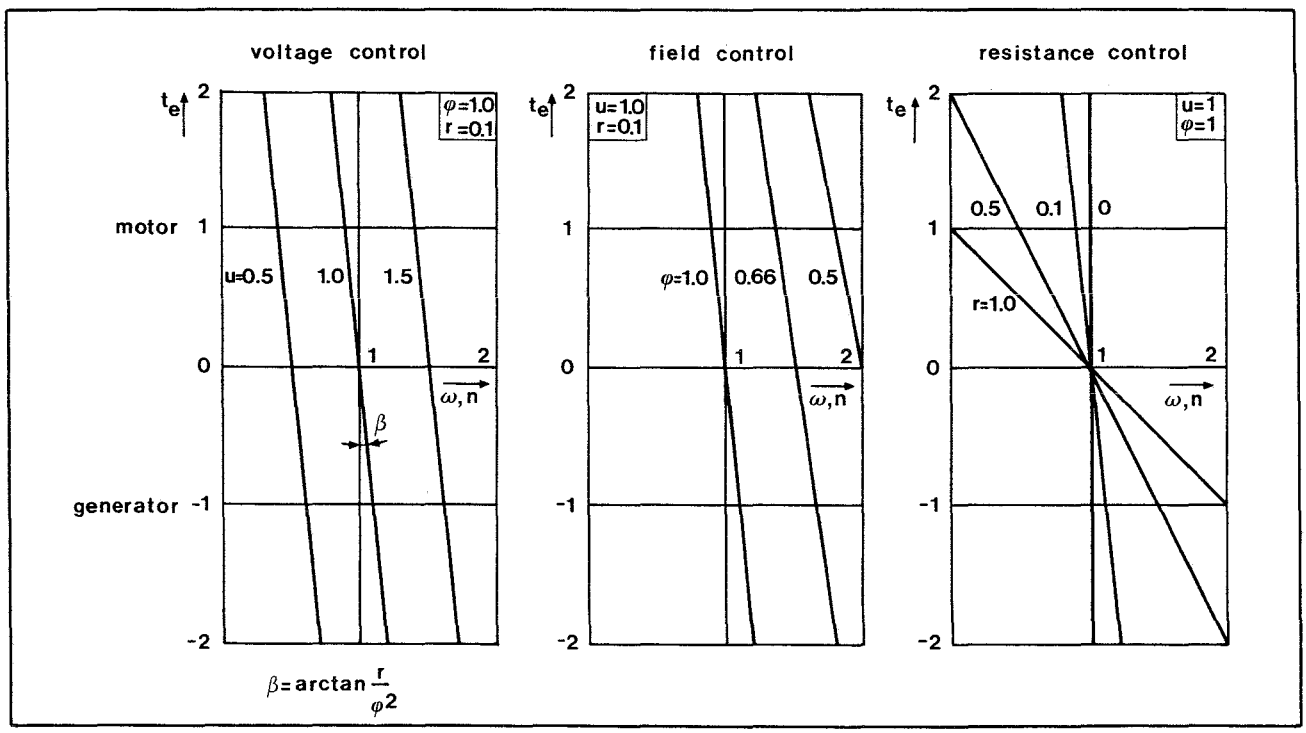

Fig. 3a Armature voltage control

Fig. 3b Field control

Fig. 3c Resistive control

Formula (12) includes three principles of affecting the torque speed curve, namely by u, φ and r. The specific influence of each of them is shown in **fig. 3a, b** and **c.**
The value r = 0,1 appears to be a quite common practice.

ad a. Speed control by armature voltage control is a very good method because of the high efficiency and the maximum torque being available at any speed. The speed range is determined by the machine parameters.

ad b. Speed control by field control offers fairly good efficiency and constant maximum output power up to high speeds, however, from very high speeds (approx. $2 \times \Omega_N$) the power is mostly limited due to commutation considerations. Compared to method **a,** field control used at voltages smaller than u = 1 will give a lower machine efficiency, because of the higher losses due to higher armature current. Besides that, the maximum power which can be converted is smaller. However, the losses in the armature controller itself are larger in a chopper than in a stepwise controller, which must be used in combination with field control, due to the fact that in the latter losses only are caused by the necessarily excitation power for electromagnetic switches. Moreover, these losses can be reduced by applying transistor choppers, such that the excitation current is limited after switching on.

ad c. Resistive speed control causes substantial energy dissipation especially at high armature current. Therefore it has a low efficiency and must be limited to the minimum.

2. SPEED CONTROL BY MEANS OF STEPWISE VOLTAGE ADJUSTMENT AND CONTINUOUS FIELD CONTROL

In the here considered drive the battery pack is devided in four blocks of 30 V each by a number of electromagnetic switches **(fig. 4).** By connecting these blocks in series and/or parallel, armature voltages of 30 V, 60 V and 120 V are obtained through which the machine speed is regulated in coarse steps. The speed can be regulated finely at each armature voltage by electronic control of the field. As the field windings are also fed from the battery pack, they had to be split in two parts in order to obtain nominal excitation current at each armature voltage.

R_v and R_p are incorporated for current limiting at low speed. Table 2 shows which switches have to be closed in a certain situation; switches which absolutely not may be closed at the same time cancel each other by normally closed interlocks.

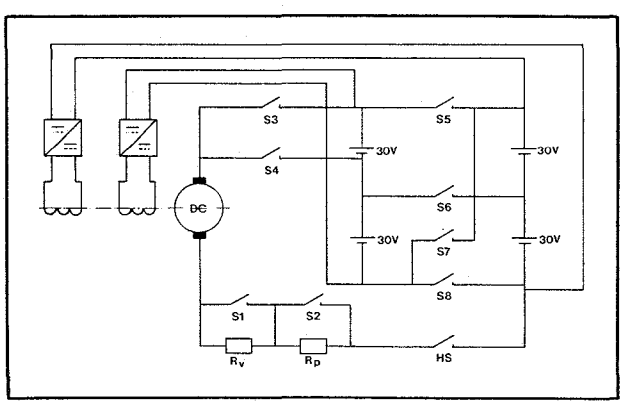

Fig. 4 Armature and field winding circuits

TABLE 2

Area	Switches in on-state								
	S1	S2	S3	S4	S5	S6	S7	S8	HS
30 V + R_v + R_p				X		X		X	X
30 V + R_v		X		X		X		X	X
30 V	X	X		X		X		X	X
60 V	X	X	X		X			X	X
120 V	X	X	X				X		X

2.1. Characteristics

The speed-torque curves for the above mentioned conditions are obtained by using (12) and the specific nominal values of the 1GV1-machine. These values are partly supplied by the manufacturer and partly determined by measurements.

$$T_{e_N} = 80\ [\text{Nm}];\ T_{S_N} = 75\ [\text{Nm}]$$

$$U_N = 124\ [\text{V}]$$

$$c_m \Phi_{a_N} = 0.54\ [\text{Wb}]$$

$$R_{a_N} = 0.83\ [\Omega]$$

$$N_{s_N} = 2200\ [\text{min}^{-1}]$$

$$R_a = 60 \cdot 10^{-3}\ [\Omega];\ r = 0.07$$

While calculating T_{e_N} no attention has been paid to the reduction of the magnetic flux Φ_a due to armature reaction and not-ideal commutation. For these reasons the effective flux will be smaller than the flux produced by the field windings only and used to derive (12).
Furthermore the torque at the machine shaft (T_S) will be smaller than T_e when the machine operates as a motor and larger when the machine operates as a generator due to iron and friction losses which depend upon speed and excitation. However, in the following we assume T_S to be linear with T_e. Furthermore nominal battery voltages are used in the characteristics and internal battery resistance is neglected.
Fig. 5 shows machine shaft torque versus machine speed and tractive effort versus car speed for armature voltages of 30 V (u = 0.24), 60 V (0.48) and 120 V (0.96) at different flux values.

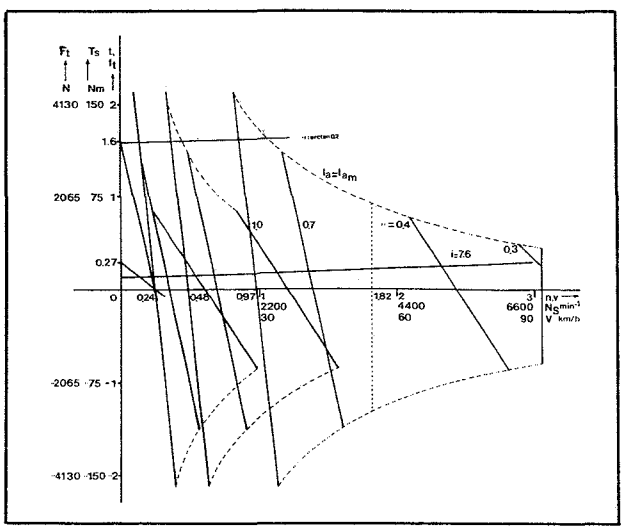

Fig. 5 Static machine characteristics and load characteristics for i = 7.6 with $\alpha = 0$ and α = arctan 0.2

Tractive effort and car speed are determined by the mechanical reduction and the wheel radius according to:

$$F_t = T_s \frac{i}{r_w} \tag{13}$$

$$V = \frac{2\pi}{60} \cdot N_s \cdot \frac{r_w}{i} \tag{14}$$

The torque is limited at all voltages by the maximum permissible armature current I_{a_M} which is constant up to $N_S = 4000$ min^{-1} ($n_S = 1.82$) and thereafter speed dependent due to the machines commutation. This dependence can be approximated by a linear function of n_S. The following equations for t_M are found.

As $|t_M| = |I_{a_M}|\,\varphi$ we get:

$$|t_M| = 2.13\,\varphi \qquad n < 1.82 \tag{15}$$

and $$|t_M| = (3.18 - 0.58n)\varphi \qquad 1.82 < n < 3.05 \tag{16}$$

The stationary load characteristics can be calculated with the wellknown formula [2]:

$$T_S = \left(\frac{1}{2}\varrho\left(\frac{2\pi}{60}\frac{r_w}{i}N_s\right)^2 A_F c_w + mg\,(f\cos\alpha + \sin\alpha)\right)\frac{r_w}{i} \tag{17}$$

The characteristic for $\alpha = 0$ and $\alpha = \arctan 0.2$ are drawn in fig. 5.

2.2. **Extra series resistors at low speeds**

In order to limit the armature current at standstill and at very low speeds to a value just high enough to produce a maximum field excitation the desired load torques, series resistors are incorporated. Two cases can be distinguished, namely:

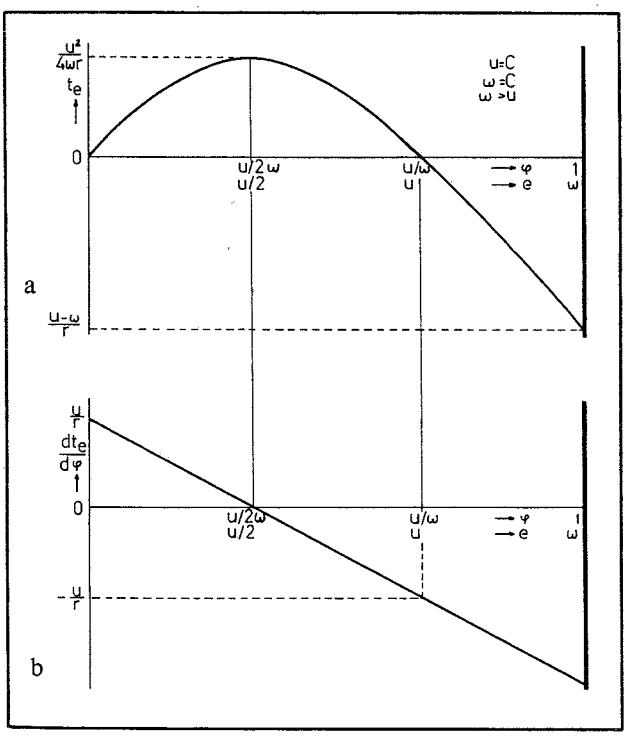

Fig. 6a EM-torque as a function of magnetic field at constant speed

Fig. 6b Transfer curve $\frac{dt_e}{d\varphi} = f(\varphi)$ at constant speed

a. Driving during a short time with a maximum torque of 120 Nm (t = 1.6), for instance in parking garages and on slopes.
b. Driving during a long time with aprox. 11 Nm (say 20 Nm; t = 0.27) while looking for a parking place or while driving in a traffic line.

The required relative resistances at standstill ($\omega = 0$) with maximum field ($\varphi = 1$) can be calculated using (12).
By taking into account the armature resistance $R_a = 0.06\,[\Omega]$ the following values for R_v and R_p are found:
$R_v = 0.065\,[\Omega]$
$R_p = 0.615\,[\Omega]$

The machine characteristics for these resistances are also shown in fig. 5. Both resistances are switched off at a machine speed of 440 min^{-1} (car speed of 6 km/h), moreover R_p is switched off when the accelerator is pushed in more then 20% ($p > 0.2$).
The switching diagram is shown in fig. 8.

2.3. **Analysis of field control at stepwise armature voltage adjustment**

In order to design a control system which is based upon field control it is essential to know certain parameters such as the transfer function $(\frac{d\,te}{d\,\varphi})$ and the position of the maximum EM-torque in the φ-n plane at different armature voltages.

2.3.1. *Quasi-stationary conditions*

For these conditions $t_e = f(\varphi)$ is analysed:

$$t_e = \frac{\varphi}{r}(u - \varphi\omega)$$

1. The zeros are found at $\varphi = 0$ and $\varphi = \frac{u}{\omega}$.

2. The maximum EM-torque will be produced when the total voltage drop across the armature circuit resistances equals the back E.M.F. :

$i_a r = \varphi\omega = \frac{u}{2}$. Its magnitude is: $t_{e_M} = \frac{u^2}{4\omega r}$.

3. The minimum EM-torque (maximum torque as generator) is limited by the maximum value of the field ($\varphi = 1$) and has a magnitude of:

$$t_{e_M} = \frac{1}{r}(u - \omega).$$

The EM-torque as a function of φ and e at constant armature voltage u is outlined in **fig. 6.** Also shown is the static transfer curve $\frac{dt_e}{d\omega} = f(\varphi, e)$.

Fig 6. shows that for small back E.M.F. (i.e. $e < \frac{u}{2}$) an increase of the field will result in higher EM-torque and for high back E.M.F. (i.e. $e > \frac{u}{2}$) in lower EM-torque.
The latter is almost always the case in motor applications of the DC-machine, however, not in the one considered here.

All points in the φ-ω plane, at which under motor conditions the EM-torque is maximum, lie on a orthogonal hyperbole which is determined by the armature voltage, i.e.

$$\varphi\omega = \frac{u}{2} = C$$

The constant C for the armature voltages 30, 60 and 120 V is respectively: 0.12, 0.24 and 0.48.
Another important factor involved, is the magnitude of the armature current which must be held within certain limits. Curves for maximum permissible armature current under motor conditions as well as under generator conditions are also orthogonal hyperboles:

$$\varphi\omega = u - i_{a_M} \cdot r \qquad (19)$$

with $i_{a_M} = \pm 2.13$ for $\omega < 1.82$

and $i_{a_M} = \pm (3.18 - 0.58\,\omega)$ for $1.82 < \omega < 3.05$

All the curves mentioned and the one for armature current equal to zero are drawn in **fig. 7** for the distinct voltage levels and armature circuit conditions.

The criteria for changeover between armature voltage levels under motor conditions differ from those under generator conditions.
– Changeover under motor conditions ($T_s > 0$):
As changeover must occur while the armature current is zero, the machine speed must be high enough to get a back E.M.F. equal to the next voltage level at maximum field ($\varphi = 1$).
This means $\omega = u$. The following values are found: (20)

$n_{30 \rightarrow 60} = 0.48$; $N_{s30 \rightarrow 60} = 1056\ \text{min}^{-1}$

$n_{60 \rightarrow 120} = 0.96$; $N_{s60 \rightarrow 120} = 2112\ \text{min}^{-1}$

– Changeover under generator conditions ($T_s > 0$):
In this case it is important to keep the breaking torque which *can* be produced as high as possible. This means that the maximum power delivered by the machine just after switching must be equal to the maximum power before switching, taking into account the field limit $\varphi = 1$ befor switching and the armature current limit $i_a = 2.13$ after.
From this it follows that:

$$n = \frac{u_H}{2} + \sqrt{\left(\frac{u_H^2}{4} + i_{a_M} r\left(\frac{u_H}{2} + i_{a_M} r\right)\right)} \qquad (21)$$

Herein is u_H the highest of the two involved armature voltages at a certain switching point.

Hence $n_{120 \rightarrow 60} = 1.05$; $N_{s120 \rightarrow 60} = 2310\ \text{min}^{-1}$
and $n_{60 \rightarrow 30} = 0.58$; $N_{s60 \rightarrow 30} = 1276\ \text{min}^{-1}$

Figure 7 gives a complete survey of the requirements of the field control system, while figure 8 shows the exact situation of switching points at certain armature circuit conditions. The following conclusions with respect to this control system can be drawn for the distinct areas:

Area I: $U = 30$ V; $R \geq 0.125\ \Omega$; $-320\ \text{A} < I_a < 320\ \text{A}$.
– The maximum permissible armature current cannot be exceeded.
– The transfer function $\frac{dt_e}{d\varphi}$ is positive except for $260 < N_s < 440$, so that the field in this range is limited according to $\varphi = -2.27.10^{-3} N_s + 1.60$.

Area II: $U = 30$ V; $R = 0.06\ \Omega$; $-320\ \text{A} < I_a < 320\ \text{A}$.
– The armature current must be limited in both positive and negative direction.

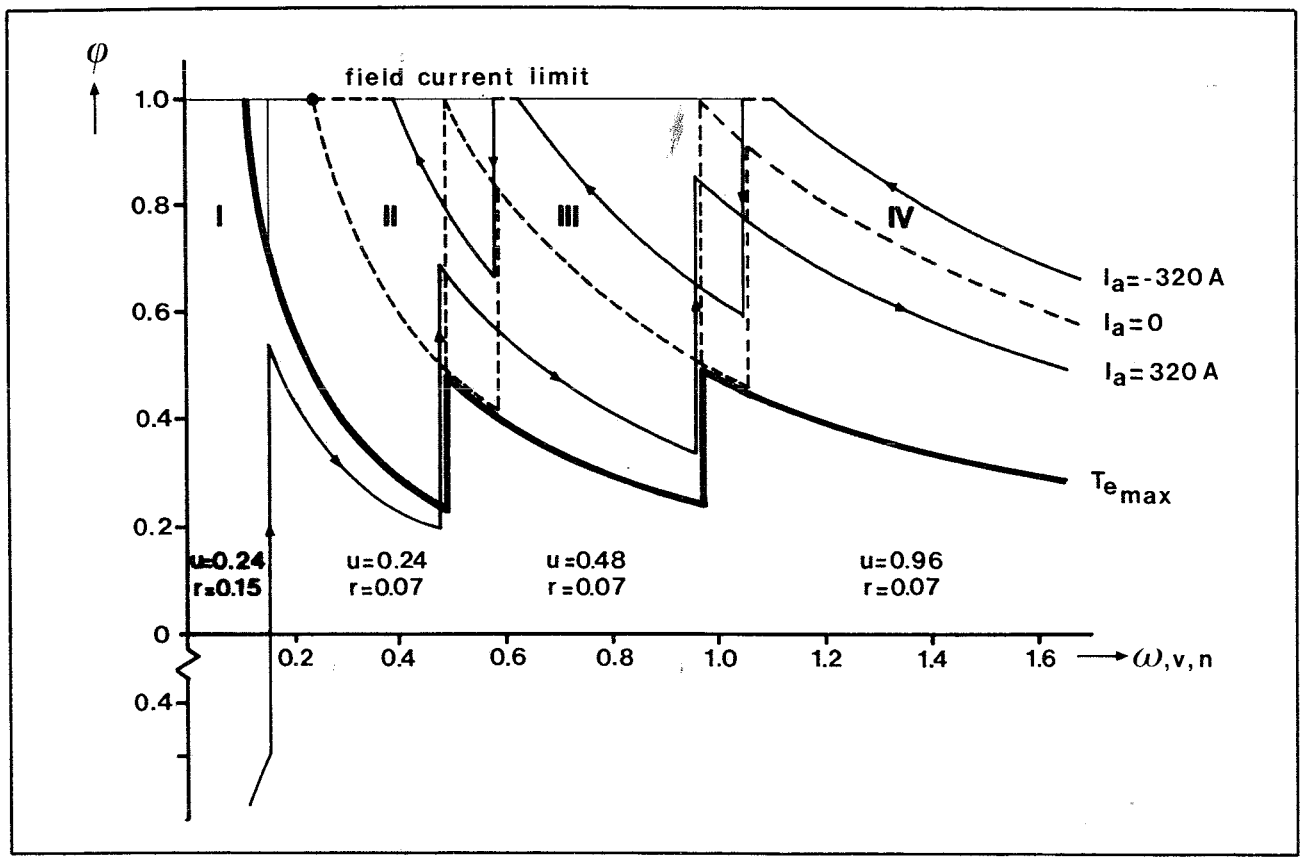

Fig. 7 Notching curves for maximum EM-torque and maximum current in the φω-plane

– In the largest part of the area the transfer function $\frac{dt_e}{d\varphi}$ is negative. During testing it appeared to be satisfactory to consider $\frac{dt_e}{d\varphi}$ negative all over the area.

Area III: U = 60 V; R = 0.06 Ω; $-320\ A < I_a < 320\ A$.
– The armature current must be limited in both directions.
– The transfer function $\frac{dt_e}{d\varphi}$ is negative all over the area.

Area IV: U = 120 V; R = 0.06 Ω; $-I_{a_M} < I_a < I_{a_M}$; $I_{a_M} = f(N)$; conditions: Identical to area III.

As the exact situation of the curves depend on the battery condition in such a way that under poor battery conditions the curve for maximum torque will possibly become higher situated in the φω-plane than the maximum motor current curve, it is necessary to take precautions in order to prevent the torque from falling to a very low value. Therefore the field in area II, III and IV is kept above the value of 0.2.

2.3.2. *The dynamic behaviour of the separately excited DC-machine with field control*

In the preceding pages field control has been regarded under quasi-stationary conditions which means that changes occur so slowly that the system, the electrical as well as the mechanical part, can follow immediately. The system behaviour under these circumstances is the most important for EV-applications, however, with respect to system design also the dynamic behaviour is important [1], [5] and [8].

The transfer function $\frac{T_e}{\varphi}$ or $\frac{T_e}{U_f}$ can only by determined for small signals around a working point due to the non-linearity of machine equations and the load characteristic. The following transfer function can be derived in the Laplace-domain, assuming a linear relationship exists between Φ_s and Φ_a.

$$H(s) = L\left\{\frac{T_e}{U_f}\right\} = \frac{-2c_1\Omega_{a_o}c_m(E_o - I_{a_o}R_a)}{2c_1\Omega_{a_o}R_a + c_m^2\Phi_o^2} \cdot \frac{(1+\frac{J}{2c_1\Omega_{a_o}}s)(1-\frac{I_{ao}L_a}{E_o - R_aI_{a_o}}s)}{(\frac{JL_a}{2c_1\Omega_{a_o}R_a + c_m^2\Phi_o^2}s^2 + \frac{JR_a + 2c_1\Omega_{a_o}L_a}{2c_1\Omega_{a_o}R_a + c_m^2\Phi_o^2}s + 1)(\frac{R_f}{L_{fo}} + s)} \quad (22)$$

Where: $\Omega_o = \frac{i}{r_w}V_o$

$E_o = c_m \Phi_o \Omega_o$

$c_1 = \frac{1}{2}\varrho A_F c_w \frac{r_w^3}{i^3}$

$J = \frac{r_w^2}{i^2}\lambda m$

λ is a constant necessary to bring into account the rotating parts of the drive. The parameters with subscript "0" refer to the chosen working point. With the wellknown techniques from control engineering it is possible to determine the response to a step input signal $U_{f\sim}$.

It appears that:
– the final value of the response has a sign *opposite* to that of $U_{f\sim}(E_o - I_{a_o}R_a)$ (see also fig. 6a.).
– the differential coefficient $\frac{dT_e}{d\tau}$ at time $\tau = 0$ has the *same* sign as that of the disturbance $U_{f\sim}$.

This means that when $E_o - I_{a_o}R_a > 0$ the system at first shows an inverse response (see **fig. 9**). The transfer function has a zero in the right part of the complex s-plane and is called a *nonminimum phase-shift transfer function.*
The physical explanation for this phenomenon is the existance of the electrical inertia of the armature, through which the transient at the beginning is determined by the field only.

3. REALISATION OF THE CONTROL SYSTEM

In principle an armature current or field control is sufficient to control speed, acceleration and regenerative breaking. However, due to the speed dependence of the field, the accelerator or brake pedal position would need to be readjusted continually in order to keep the desired acceleration or deceleration. By applying an extra torque control loop, the driving or breaking torque is kept constant as far as the armature or field current limits are not exceeded.

In the area where the series resistors are incorporated in the armature circuit and hence $\frac{dt_e}{d\varphi} > 0$, the field is controlled straightaway by the accelerator pedal signal. Fig. 10a, and b shows the block diagrams of the distinct control systems.

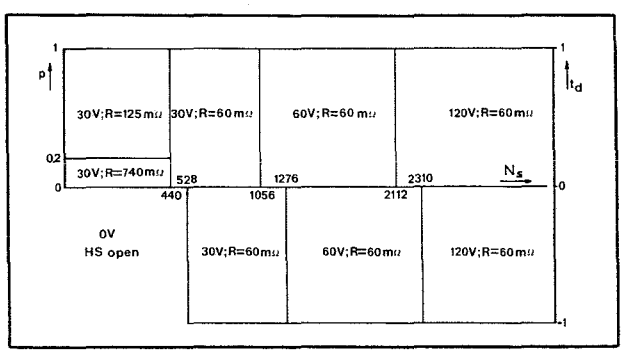

Fig. 8 Switching diagram

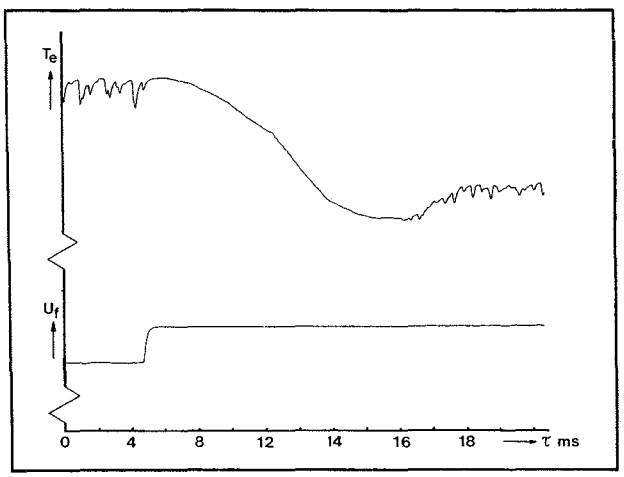

Fig. 9 Torque response to step input field winding voltage

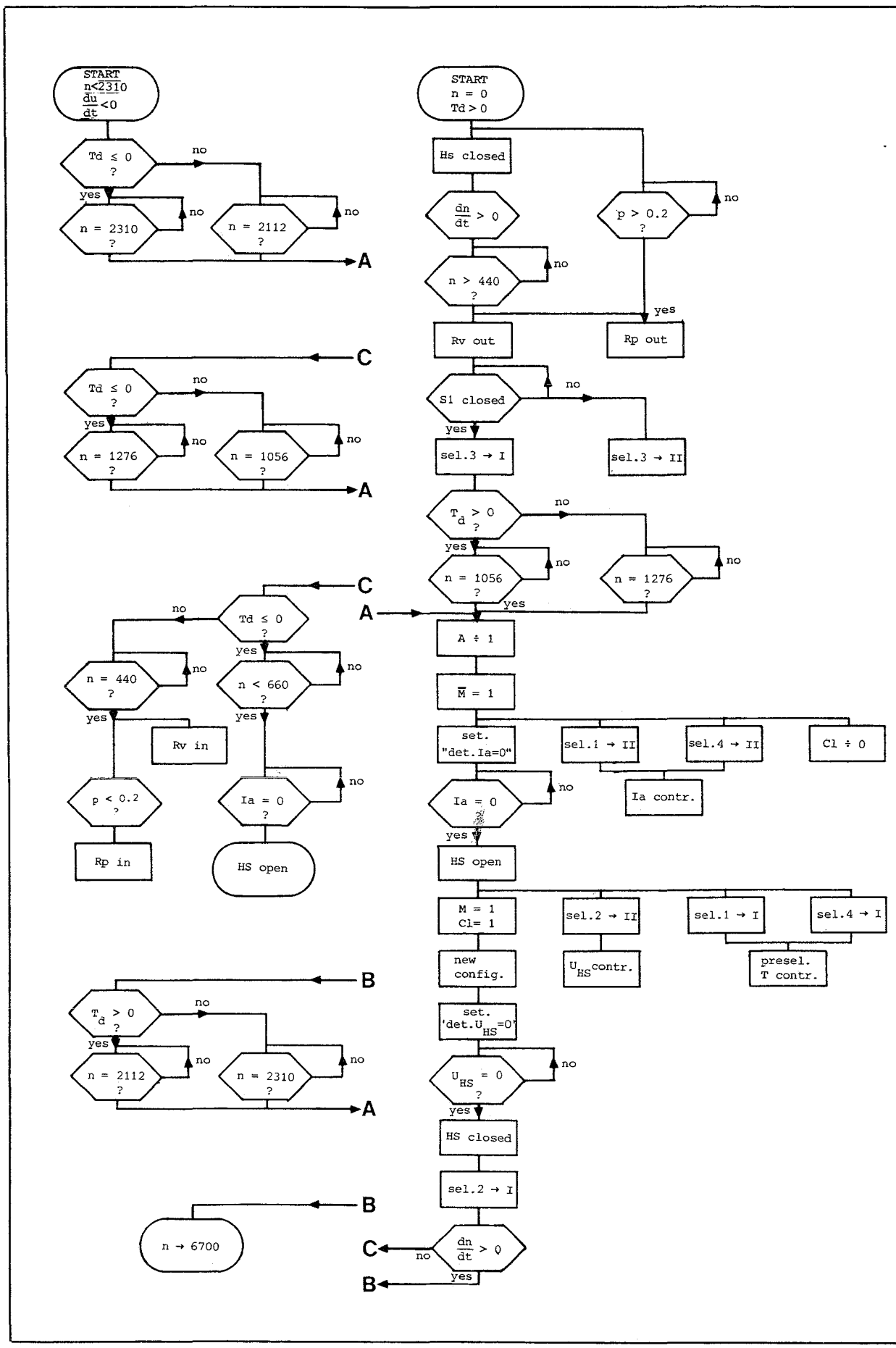

Fig. 14 Flow chart for accelerating and decelerating

3.1. Field current controllers

The field current controllers are two-quadrant choppers implemented with power MOSFETs (see **fig. 11a**). Due to the fact that the excitation voltage can be reversed, current changes can be accomplished with the same speed in both directions (see **fig. 11b**).

For a fast decrease of the field current, the energy stored in the field windings will be fed back into the battery via the diodes D1 and D2. The frequency of the PWM-signal is 400 Hz which is high enough to get a smooth current at a given field coil time constant of 100 ms.
The average excitation voltage and, under stationary conditions, also the average current is proportional to the control voltage applied to the PW-modulator (**fig. 11c**).

3.2. Measurement of the field

Due to the saturation of the magnetic circuit and hence non-linear relation between I_f and Φ_s, the field current cannot be used straightaway to determine the instantaneous EM-torque. Although, if the hysteresis is neglected, this function can be approximated quite accurately using the method of least squares, in practise it appeared to be satisfactory to make an even coarser approximation with three straight lines which remain all within the hysteresis curve (**fig. 12**).
Based upon this approach the flux value is obtained electronically from the field current.

4. FLOW CHART AND BLOCK DIAGRAM OF VOLTAGE ADJUSTING AND FIELD CONTROL SYSTEM

In order to change armature voltage under no-current conditions the current before *opening* the main switch and the vol-

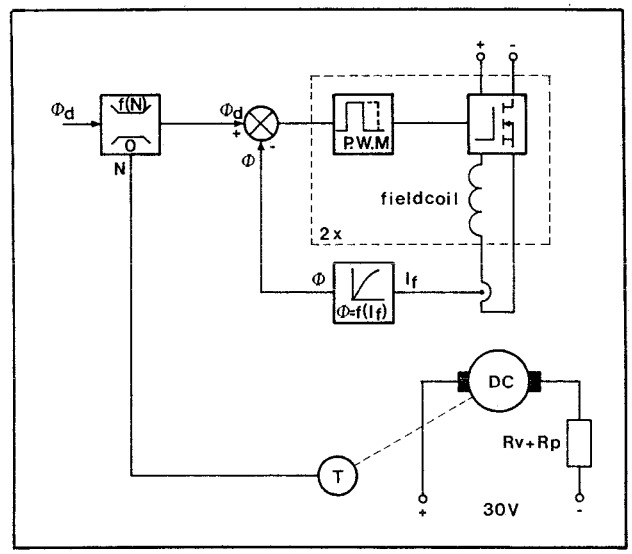

Fig. 10a Field control in the area U = 30 V; R ≥ 125 mΩ

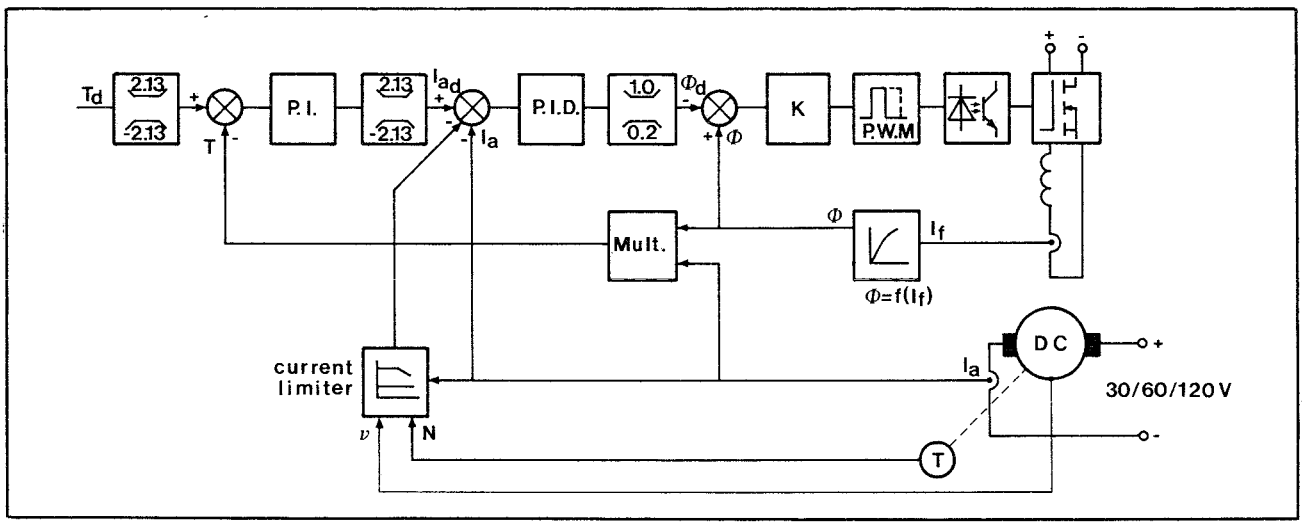

Fig. 10b Torque control in the areas U = 30, 60 and 120 V; R = 60 mΩ

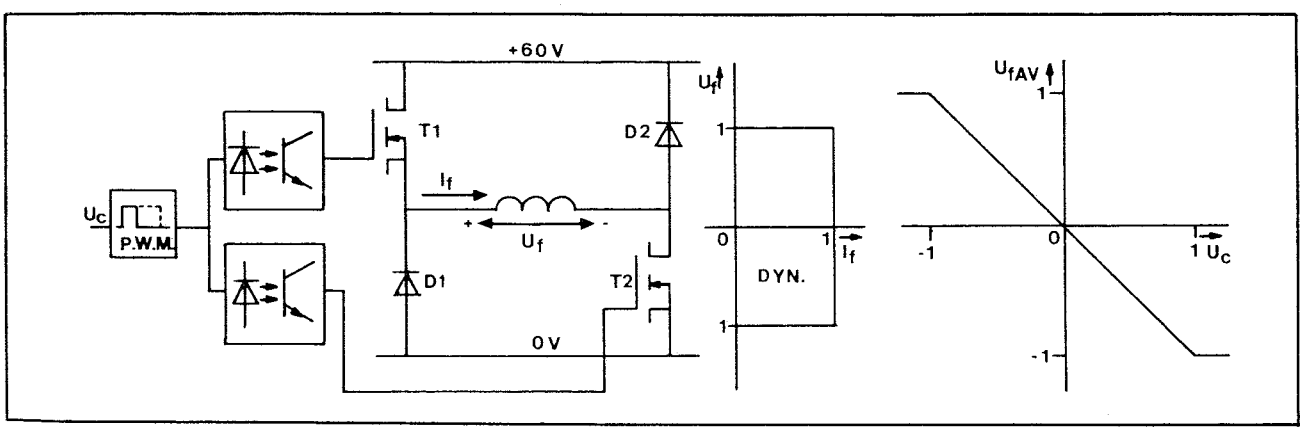

Fig. 11a Field current chopper

Fig 11b Two quadrant operation

Fig. 11c Excitation voltage vs. control voltage

Fig. 15 Block diagram

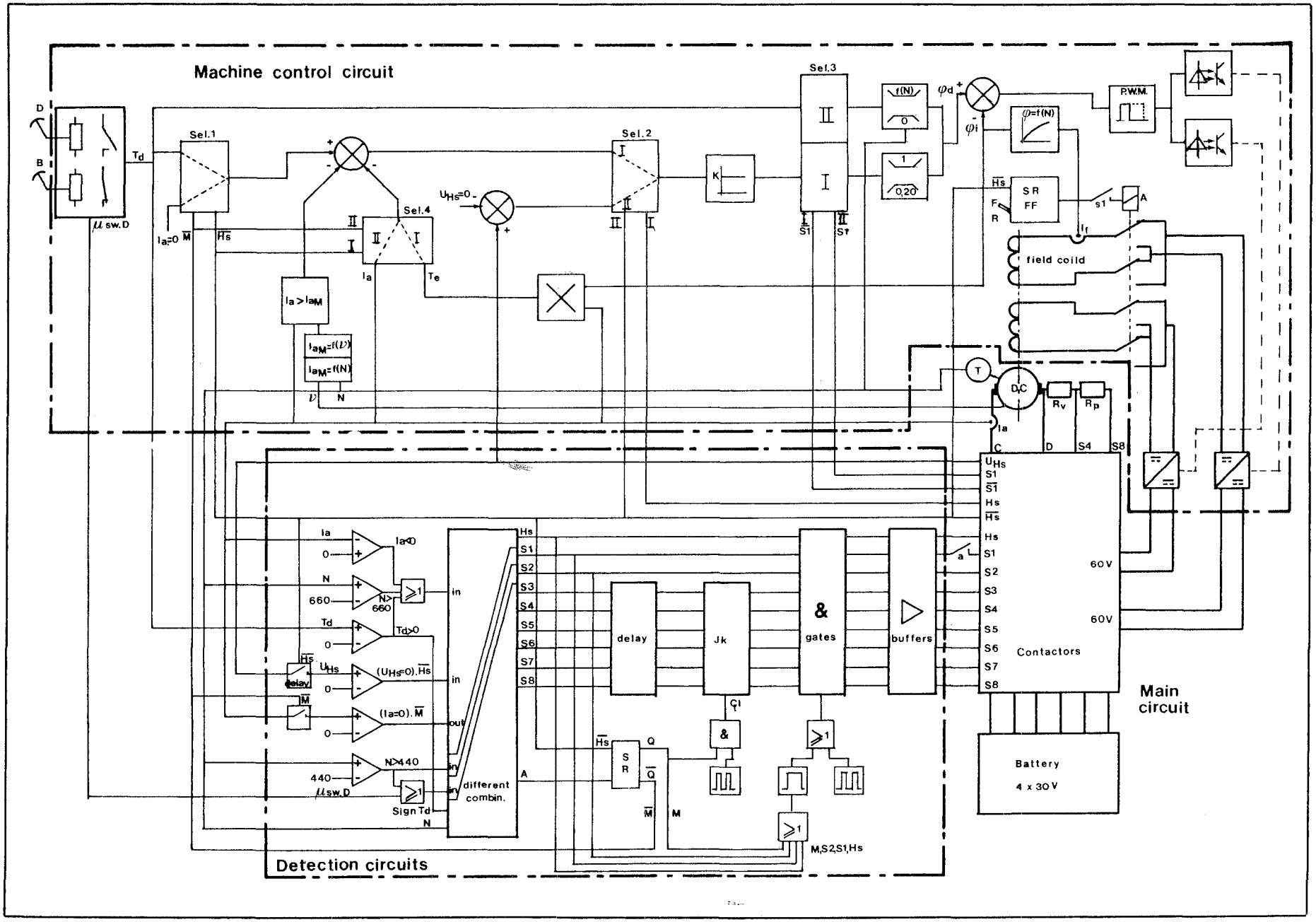

tage across the main switch before *closing* it in the new state, are forced to zero.
Due to this program the field control operates successively under torque-, current-, and voltage control. The entire program is a complex structure which can best be understood by following the flow chart of **fig. 14,** together with the block diagram of **fig. 15. Fig. 13** shows the voltage across the main switch, the armature current and the field current during switching.

5. CONCLUSIONS

The conclusions drawn from the obtained test-bench results can be summarized as follows.
– It is possible to build a convenient speed control based upon a conventional circuit concept with use of modern control electronics.
– The control concept is probably very suitable to implement with microprocessor technology, which means that prices can be acceptable in larger series.
– The relatively low torque-armature current ratio, due to the field weakening, can be regarded as a disadvantage of this speed control.

6. ACKNOWLEDGEMENTS

The author wishes to express his thanks to professor J.A. Schot for reading the manuscript and to acknowledge his gratitude to Messrs. Barten, v. d. Boomen and Kremer, who are responsible for much of the realisation of this project.

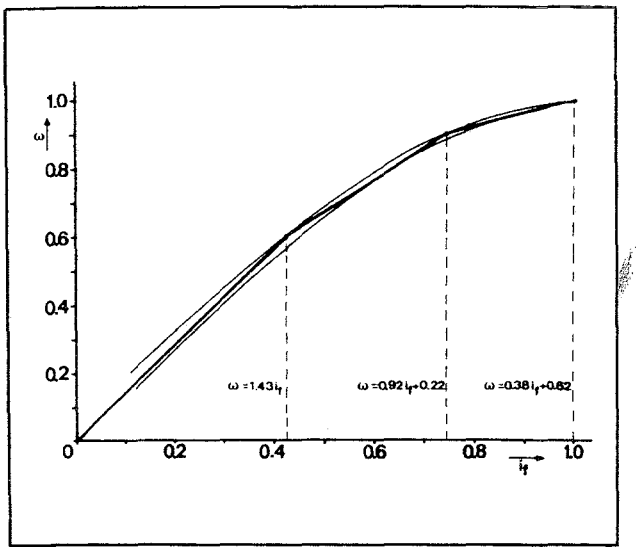

Fig. 12 Linear approximation of $\Phi_s = (I_f)$

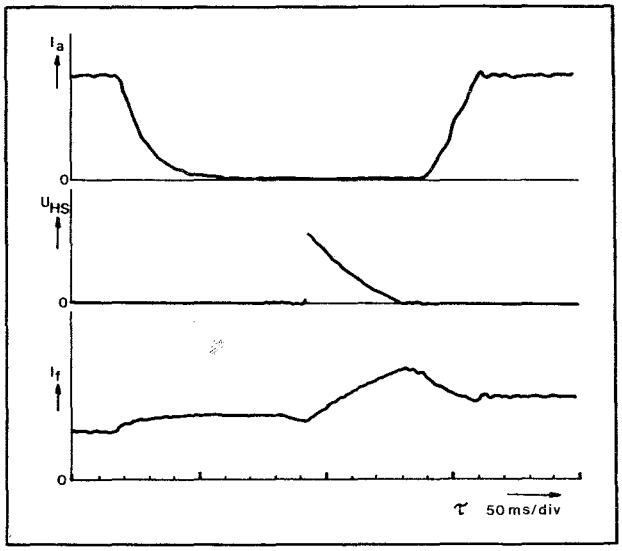

Fig. 13 Armature current, voltage across main switch and field current vs. time during switching to a higher voltage

LIST OF SYMBOLS AND SUBSCRIPTS

A_F Front surface of car.
c_m Machine constant.
c_w Streamline constant.
E Back E.M.F.
e Normalized E.M.F.
F_t Tractive effort.
f Friction constant.
g Gravity constant.
H(s) Complex transfer function.
HS Main switch.
I_a Armature current.
I_f Excitation current.
i_a Normalized armature current.
i Mechanical reduction.
J Mechanical inertia.
L_a Armature inductance.
L_f Field coil inductance.
m Mass of the vehicle.
N_s Machine shaft speed.
p Accelerator position.
R Total armature circuit resistance.
R_a Armature resistance.
R_f Field coil resistance.
R_N Nominal armature resistance $\frac{U_N}{I_{a_N}}$.
R_p Parking resistor
R_v Series resistor.
r Normalized armature circuit resistance.
r_w Wheel radius.
S Switch.
s Laplace operator.
T_s Machine shaft torque
T_e Electromagnetic torque.
T_{fr} Friction torque.
T_L Load torque.
t_e Normalized EM-torque.
U Armature voltage.
U_b Voltage drop across brushes.
U_f Field coil voltage.
u Normalized armature voltage.
V Vehicle speed.
v Normalized vehicle speed.
α Slope angle.
λ Constant.
ν Field winding temperature.
ϱ Specific air density.
τ Time.
Φ_a Enclosed stator flux.
Φ_s Stator flux.
φ Normalized flux $\frac{\Phi_a}{\Phi_N}$
ω Normalized angular speed.
Ω_s Angular machine shaft speed.

Additional subscripts

AV Average value.
L Laplace domain.
M Maximum.
m Minimum.
N Nominal.
o Working point.
$\sim$ Small signals.

REFERENCES

[1] Cool, J. C., Schijf, F. J. Viersma, T. J., Regeltechniek. Elsevier, Amsterdam/Brussel 1979.

[2] Dongen, L. A. M. van, 'Aandrijflijnen voor elektrische voertuigen' Rapportnr. WV 155-043, T.H. Eindhoven 1979.

[3] Dongen, L. A. M. van, Graaf, R. van der, 'The Eindhoven Experimental Vehicle: Vehicle Design and Drive Train', Drive Electric Amsterdam 1982.

[4] Dongen, L. A. M. van, Graaf, R. van der, Visscher, W. H. M., 'Theoretical Prediction of Electric Vehicle Energy Consumption and Battery State-of Charge During Arbitrary Driving Cycles', EVC No. 8115, EVC Symposium VI Baltimore, Maryland

[5] Dorf, R. C., Modern Control Systems, third edition. Addison-Wesley, Reading Massachusetts 1980

[6] Jong, H. C. J. de, Kreek, J. van der, 'De statische karakteristieken van de gelijkstroomcommutatormachine' Lecture notes EM-3615-0, group Electromechanics, T.H. Eindhoven

[7] Koumans, W. A., 'Electric car project of the Eindhoven University of Technology' PPL Conference Publication number 14, pp 87-90

[8] Pfaff, G., Reglung Elektrischen Antriebe I: Eigenschaften, Gleichungen und Strukturbilder der Motoren R. Oldenbourg Verlag, München und Wien 1971

[9] Siemens, A. G., Gleichstrom-Fahrmotor 1GV1: Technische Beschreibung.

[10] Visscher, W. Dongen, L. A. M. van, 'Battery State-of Charge Model for Driving Cycle Operation'. Drive Electric Amsterdam 1982